Climate Dynamics
https://doi.org/10.1007/s00382-018-4329-6

Global diurnal temperature range (DTR) changes since 1901

Xiubao Sun[1,2,3] · Guoyu Ren[2,3] · Qinglong You[1] · Yuyu Ren[3] · Wenhui Xu[4] · Xiaoying Xue[2,3] · Yunjian Zhan[4] · Siqi Zhang[3] · Panfeng Zhang[2]

Received: 7 January 2018 / Accepted: 24 June 2018

Abstract
Previous observational analyses show that the land-surface diurnal temperature range (DTR) has decreased in the past 6 decades worldwide. Based on a newly developed China Meteorological Administration–Land Surface Air Temperature (CMA-LSAT) dataset, we analyzed the DTR changes between 1901 and 2014. Results indicate that the global land surface DTR significantly decreased at a rate of −0.036 °C decade^{-1} over the 1901–2014 period, mainly due to the large decrease in DTR from 1951 to 2014. For the first half of the twentieth century, most grid boxes (spatial resolution 5° × 5°) show a positive DTR trend, with the positive trends of 32.4% grid boxes being statistically significant, leading to a large and significant increase of 0.048 °C decade^{-1} in DTR. However, a dramatic reversal in DTR change occurred in early 1950s, with most parts of global lands exhibiting a shift from increasing to decreasing trends. The global land average DTR decrease during 1951–2014 was −0.054 °C decade^{-1}, with 45.0% grid boxes showing significant negative trends. The reverse phenomenon is more obvious in the Northern Hemisphere than that in the Southern Hemisphere. For the periods 1979–2014 and 1998–2014, the decreasing trends in DTR mainly occur in the Northern Hemisphere. The DTR in the Southern Hemisphere experienced much larger increases during the two recent periods than during the period 1951–2014. Asia, Eastern North America, and Australia exhibited widespread decreases in DTR, although the trend pattern for global DTR is generally mixed during 1979–2014 and 1998–2014. There is a good negative correlation between DTR and precipitation in the Northern Hemisphere from 1901 to 2014, with a correlation coefficient of −0.61. The change in precipitation and number of volcanic eruptions, and the "early brightening" of Europe (Stockholm) all benefit the increase of DTR at global and regional scales in the first half of the twentieth century.

Keywords DTR · Trends · Maximum temperature · Minimum temperature · Global lands

1 Introduction

Diurnal temperature range (DTR) is an important indicator of climate change in the past century and can provide more information than mean temperature alone (Braganza et al. 2004). The changes in DTR can directly reflect the consistency of the maximum and minimum temperature changes. The Fifth Assessment Report of the Intergovernmental Panel on Climate Change (IPCC AR5) indicated a much smaller warming rate of maximum temperature (T_{max}) than minimum temperature (T_{min}), but mean temperature (T_{mean}) has almost certainly shown a significant increasing trend since 1950, at a warming rate of more than 0.1 °C decade^{-1} (IPCC 2013). On the global scale, previous studies have indicated a warming rate of T_{min} approximately twice that of T_{max} since 1950, which has directly caused the significant large-scale decreasing trends in the global and hemispheric mean

✉ Guoyu Ren
guoyoo@cma.gov.cn

[1] College of Atmospheric Science, Nanjing University of Information Science and Technology (NUIST), Nanjing 210044, China

[2] Department of Atmospheric Science, School of Environmental Studies, China University of Geosciences (CUG), Wuhan 430074, China

[3] Laboratory for Climate Studies, National Climate Center, China Meteorological Administration (CMA), Beijing 100081, China

[4] National Meteorological Information Center, China Meteorological Administration (CMA), Beijing 100081, China

Published online: 28 June 2018

DTR (e.g. Karl et al. 1993; Easterling et al. 1997; Alexander et al. 2006; Vose et al. 2005; Wang et al. 2014; Thorne et al. 2016).

On the regional scale, the DTR in some countries and regions, including America (Karl et al. 1993; Powell and Keim 2014), Europe (Klein Tank and Können 2003; Hundecha and Bárdossy 2005; Makowski et al. 2009; Jaagus et al. 2014; Río et al. 2012), China (Zhai and Pan 2003), Canada (Zhang et al. 2000), and Hindu Kush-Himalaya region (Sun et al. 2017a), has also shown a significant decreasing trend. In contrast, both T_{max} and T_{min} have shown synchronous variations in some other countries and regions, resulting in no significant change in DTR in these countries and regions, including India (Kumar et al. 1994), New Zealand (Salinger and Griffiths 2001), and parts of Africa (Samba and Nganga 2014). On the seasonal scale, Vose et al. (2005) found that the DTR has decreased in all seasons on the global and hemispheric scales, especially in December–February and September–November. Besides these interdecadal variations, previous studies have also found that the global DTR shows a remarkable reversal phenomenon, but with different reversal periods. Makowski et al. (2008) found that the long-term decreasing trend of the DTR in Western Europe began to reverse in the 1970s, while the reversal phenomenon in Eastern Europe occurred in the 1980s. Based on a climate model, Easterling et al. (2006) found that the global DTR will decrease until 2035, but will change to no real trend from 2035 to 2100. Zhou et al. (2009) investigated DTR as simulated by 11 AOGCMs models since 1900 and indicated that the global DTR will decrease by 0.30 °C from 1900 to 2099. However, climate models cannot simulate the actual DTR changes very well.

Overall, despite the different study periods and scales, most previous studies concur in finding a decrease in the global DTR over the past few decades. Furthermore, the trend of global and regional DTR simulated by climate models is obviously smaller than the trend detected from observation.

Dai et al. (1997, 1999) investigated the causes of the decreasing DTR and found that clouds, soil moisture, and precipitation can reduce DTR by 25–50% compared with clear-sky days over most land areas, while atmospheric water vapor has a small effect on DTR. Stone and Weaver (2002) also found that decreasing DTR in model simulations tends to be associated with changes in cloud cover and soil moisture. Zhou et al. (2008, 2009) analyzed the reasons for the obvious DTR reduction in dry regions and found that vegetation removal and reduced soil radiation can reduce DTR during periods of drought in semi-arid regions. Furthermore, long-term variations in solar radiation reaching the surface cause much of the observed decadal DTR variability (Wild et al. 2005, 2007; Shen et al. 2015; Wang et al. 2013). Easterling et al. (1997) indicated that atmospheric aerosol levels in the Southern Hemisphere (SH) were lower than those in the Northern Hemisphere (NH), which contributed to the different decreasing rates in hemispheric DTR. In addition, urbanization effects are also considered to be another major reason for decreasing global and regional DTR (e.g. Ren et al. 2006, 2014; Wang et al. 2012; Zhou and Hansen 2004; Zhou and Ren 2011).

Owing to the poor spatial coverage of daily observation data, most previous research into the characteristics of DTR changes begin in 1951 (e.g. Karl et al. 1993; Easterling et al. 1997; Vose et al. 2005). Recent studies have increased the global coverage rates of the last decades from 54% (Easterling et al. 1997) to 71% (Vose et al. 2005).

However, there are a few outstanding problems in global T_{max}, T_{min}, and DTR research that need to be addressed. These include: (1) what is real change in first half of the twentieth century, and what is the overall DTR trend of the whole twentieth century? These questions have not yet been understood due to the poor quality of the observations; (2) what are the possible reasons for the different changes in early and late twentieth century? And what is the main reason for the 1950s reversal phenomenon? (3) do T_{max} and T_{min} have 'diurnal asymmetry' changes in the first half of twentieth century, and what is the possible reason of the diurnal asymmetry?

To address these issues, we use the newly developed, global-scale, China Meteorological Administration–Land Surface Air Temperature (CMA-LSAT) dataset (Sun et al. 2017b; Xu et al. 2017) in the present study to analyze the characteristics of DTR change since 1901, and we are able to obtain a few of interesting results with emphasis on the early 1950s reversal phenomenon.

2 Data and methods

The source of the monthly mean temperature used in the current analysis is the CMA-LSAT dataset, which includes 10,240 stations with a record length of 114 years (1901–2014) and a quality control and homogenization procedure reported previously in the literatures (Sun et al. 2017b; Xu et al. 2017). Compared with the other existing global land surface air temperature datasets, this new dataset shows similar ability in describing global temperature changes, despite there are some differences when describing regional temperature changes (Xu et al. 2017). Nonetheless, this problem is considered to have little influence on the results. The complete dataset contains monthly T_{max} and T_{min} values for 7999 and 7381 stations, respectively (Sun et al. 2017b; Xu et al. 2017).

In this study, we select only those stations that have at least 15 years of records in the base period 1961–1990, and at least 2 years of records in every 10 years during the base

period. We also consider the problem of missing data by discarding the annual value with monthly records of less than 6 months in calculating the annual temperature anomalies. Ultimately, we obtain a dataset consisting of monthly T_{max}, T_{min}, and DTR for 4664, 4447, and 4399 stations, respectively, for use in our analysis. The spatial distribution and record lengths of the stations are shown in Fig. 1a. Clearly, there is better spatial coverage of stations and grid boxes in the Northern Hemisphere (NH) than in the Southern Hemisphere (SH). Stations with record lengths of more than 100 years are mainly concentrated in Europe, North America, Japan, and Australia. Areas with low spatial coverage are Africa, South America, Antarctica, and high latitudes in the NH. The spatial distribution of stations is generally consistent with that used in the study by Vose et al. (2005).

China Meteorological Administration- Global Historic Precipitation dataset (CMA-GHP) (Yang et al. 2016) is used to calculate the changes in the precipitation in the NH from 1901 to 2014. The local and discontinuous properties of precipitation data are taken into account, and we select only those stations that have at least 60 years of records. Finally, 412 NH precipitation grid boxes (5°×5°) corresponding to those of the DTR data are selected to calculate the NH precipitation series.

We construct both the NH and SH time series using the method of Jones et al. (2001). First, each hemisphere is divided into grid boxes with a spatial resolution of 5°×5°, and each grid box has at least one station. The grid boxes used for the estimation of regional average are shown in Fig. 1b (the purple areas). Then, gridding of the temperature anomalies is carried out by averaging all values within the 5°×5° grid boxes. Finally, the time series are constructed by area-weight averaging all the grid boxes with data using the cosines of the central latitudes of the grid boxes as weight coefficients. A global annual anomaly time series is obtained by combining the Southern and Northern Hemisphere time series with a weighting coefficient of 1:2 (Jones and Moberg 2003).

The double-end (Start and end year) moving linear trend (DEMLT) refers to the moving linear trend with a fixed step but with double ends of the sub-series displayed backwards over time. In this study, the DEMLT is calculated for 30- and 50-year steps. Such a moving linear trend analysis method has also been used in previous studies (Ren et al. 2015; Fyfe et al. 2016).

Annual mean values are those from January to December. The linear trends of the anomaly series are obtained using the least-squares method to calculate the linear regression coefficients between temperature and ordinal numbers of time (e.g. $i = 1, 2, 3 \ldots 114$ for 1901–2014). The significance of the linear trends of the temperature series is judged using the two-tailed Student's t test. In this study, a trend is considered statistically significant if it is significant at the 5% ($P < 0.05$) confidence level. The MK test and polynomial fitting are used to detect the trend change and abrupt point of the global DTR series.

3 Changes in global DTR

3.1 Long-term time series

Global and hemispheric annual T_{max}, T_{min}, and DTR anomaly long-term time series from 1901 to 2014 are shown in Fig. 2a–c, respectively. It can be seen that the warming rate of global and hemispheric T_{min} was larger than that of T_{max} during 1901–2014, which suggests that the decreasing trend of DTR for the entire study period can be attributed to stronger increases in T_{min} (Fig. 2a, b). Global DTR showed obvious decreasing trends after the 1950s (Fig. 2c). During

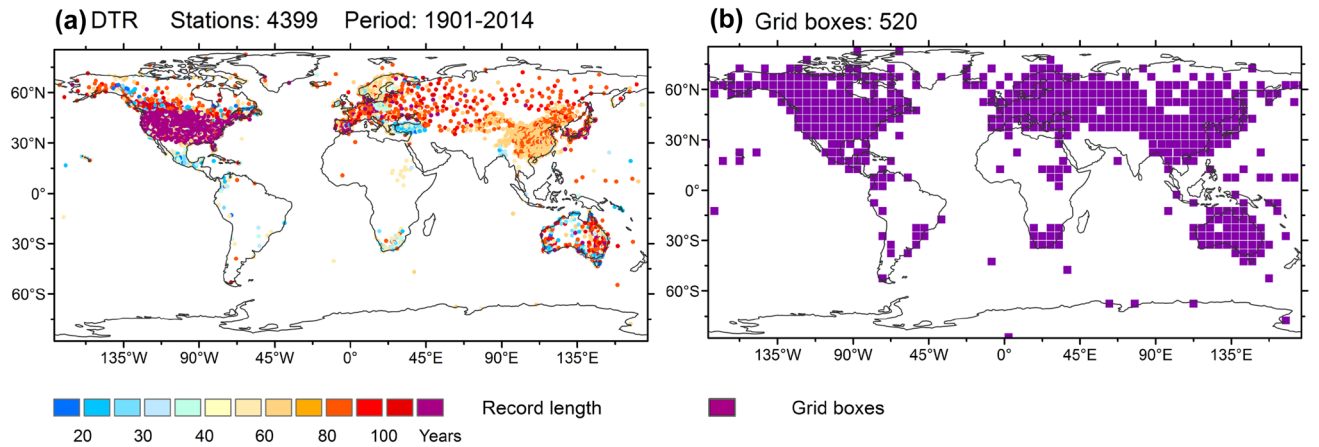

Fig. 1 Distribution of global observation stations from 1901 to 2014 (**a**) and the grid boxes at a spatial resolution of 5°×5° used in this work (**b**). Color points in **a** indicate the different record length of the data

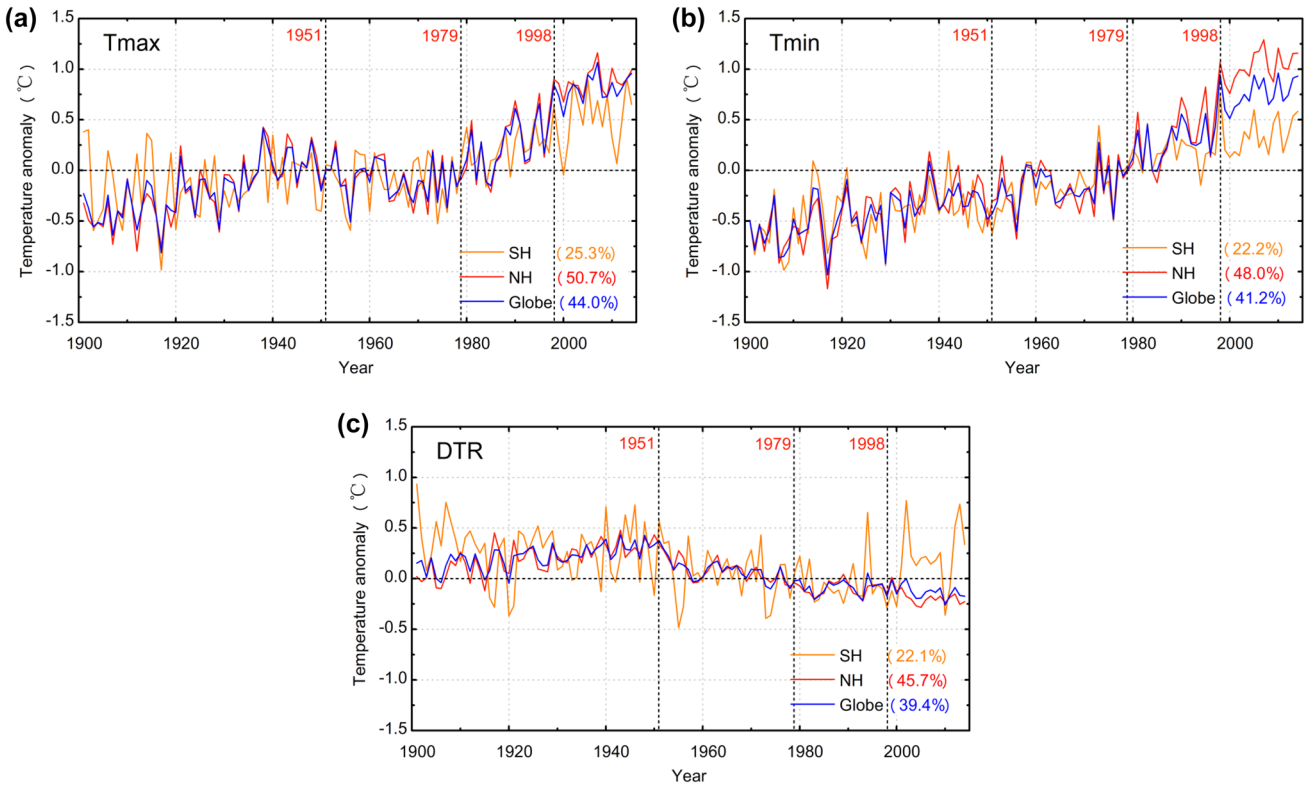

Fig. 2 Annual mean **a** T_{max}, **b** T_{min}, and **c** DTR anomaly series for the global (blue curves) and NH and SH (red and orange curves, respectively) between 1901 and 2014 relative to 1961–1990. Percentages in parentheses indicate station coverage

the late 1970s to 2000, T_{max} and T_{min} exhibited a similar variation pattern with the change of T_{mean}, and showed a dramatic increasing trend. Furthermore, we find that both T_{max} and T_{min} consistently showed a warming slowdown from 1998 (2000), which is also in agreement with the recently reported regional and global warming hiatus phenomenon (e.g. Sun et al. 2017b, c; Kerr 2009; Fyfe and Gillett 2014; Li et al. 2015).

Figure 2c shows the global and hemispheric DTR anomaly series. During 1901–1951, the global DTR series shows an increasing trend with positive anomalies in most years. In the early 1950s, a remarkable reversal phenomenon occurred in DTR, when it changed from increasing to decreasing in most parts of the world. After 1951, in general, DTR showed a decreasing trend. However, there were also slight reversal phenomena between 1951 and 2014. DTR shows an obvious and consistent decreasing trend in 1951–1983 and 2000–2014, but a slight increasing or stable trend during 1984–2000. The pattern of changes during 1951 to the 2000s agrees with previous studies by Easterling et al. (1997), Vose et al. (2005) and Thorne et al. (2016). All of the above analyses reveal that three reversal phenomena occurred in the past century. A remarkable reversal phenomenon occurred in the early 1950s, while slightly weaker reversal phenomena occurred in the 1980s and 2000s.

3.2 Heterogeneity of change rates

The change rates of T_{max} and T_{min} for the globe and the two hemispheres in different periods are shown in Fig. 3a, b. For the entire study period, the results clearly reveal that both global T_{max} and T_{min} decreased by nearly 1.1 and 1.6 °C between 1901 and 2014, respectively. The warming rate of T_{min} (0.142 °C decade^{-1}) is approximately 1.5 times that of T_{max} (0.1 °C decade^{-1}). T_{max} and T_{min} showed a more obvious warming trend during 1979–2014, and the global T_{max} and T_{min} increases occurred at rates of 0.284 °C decade^{-1} and 0.301 °C decade^{-1}, respectively. The warming rates of T_{max} and T_{min} in the first half of the twentieth century were obviously lower than those in the second half of the twentieth century. The warming rates in the NH are larger than those in the global and SH for different periods. For 1998–2014, the change rates of global T_{max} and T_{min} were 0.098 °C decade^{-1} and 0.119 °C decade^{-1}, respectively. Remarkably, all of the trends in the period 1998–2014 are not significant ($P < 0.05$), with a higher level of uncertainty (black error bars in Fig. 3a, b), probably because of the sensitivity of trend estimates to the length of a series.

The changes rates of DTR for the globe and the two hemispheres in different periods are shown in Fig. 3c. The DTR in the NH, SH, and globe consistently decreased by nearly

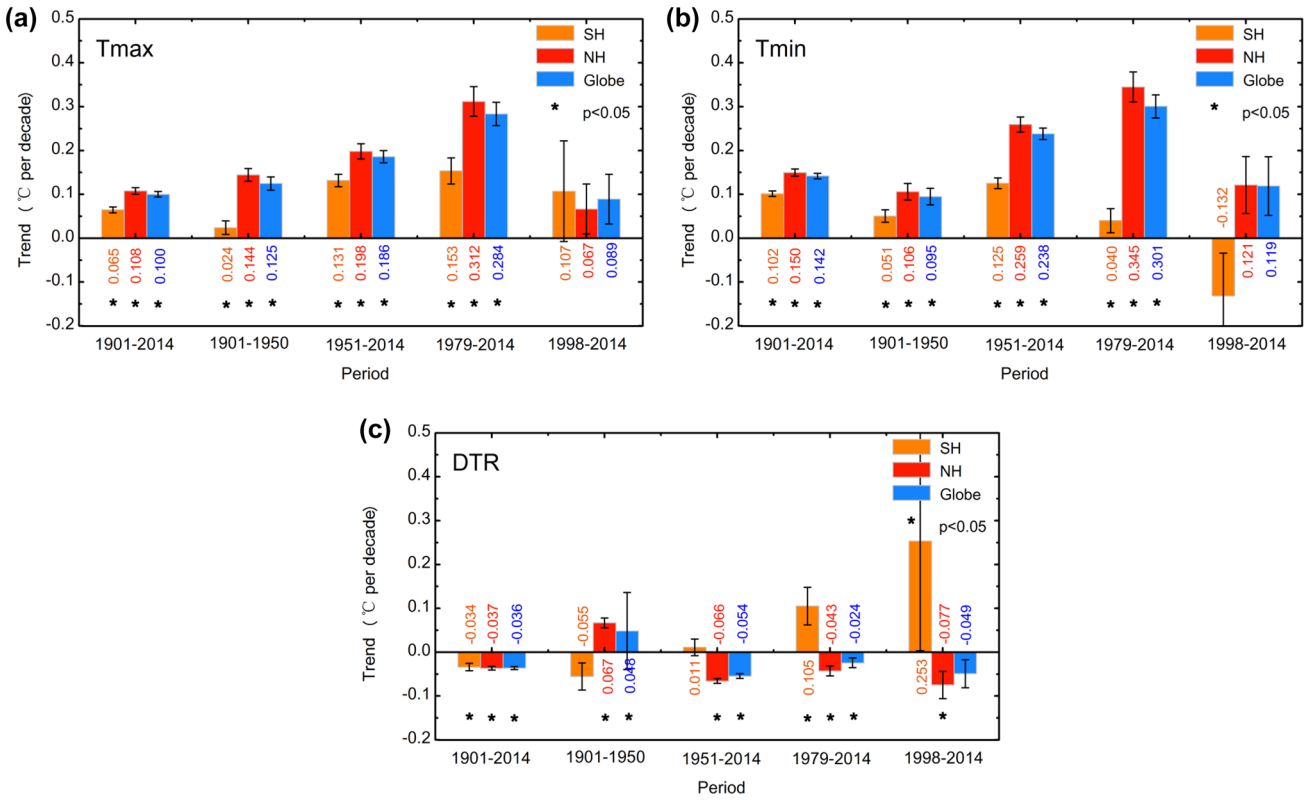

Fig. 3 Hemispheric and global **a** T_{max}, **b** T_{min}, and **c** DTR trends in different periods [1901–2014, 1901–1950, 1951–2014, 1979–2014, and 1998–2014]. Numbers in different colors indicate the rates of change. Error bars indicate 2 times the standard deviation. Statistically significant ($P < 0.05$) trends are marked with asterisks

0.4 °C between 1901 and 2014. The decreasing trend of DTR was slightly larger in the NH (−0.37 °C decade^{-1}) than in the SH (−0.34 °C decade^{-1}). In the first half of the twentieth century, global DTR showed a significant increasing trend (0.046 °C decade^{-1}), NH DTR showed a dramatic increasing pattern (0.067 °C decade^{-1}), and SH DTR shows a statistically insignificant decreasing trend (−0.055 °C decade^{-1}). In the second half of the study period, the trend of DTR showed obvious reversal phenomenon, and the trends of global, NH, and SH DTR were −0.054, −0.066, and 0.011 °C decade^{-1}, respectively. Therefore, the downward trend of DTR between 1901 and 2014 was mainly due to the large decreased DTR from 1951 to 2014. For 1979–2014 and 1998–2014, the global (−0.049 °C decade^{-1}) and NH (−0.077 °C decade^{-1}) DTR showed an obvious decreasing trend, while the SH showed a statistically insignificant ($P < 0.05$) increasing trend with a high level of uncertainty.

The double-end moving linear trends (DEMLTs) with 30- and 50-year fixed steps more clearly display the temporal evolution of the long-term temperature trends. The 30-year DEMLT for the annual mean T_{max}, T_{min}, and DTR for the globe are shown in Fig. 4a. A negative DTR DEMLT appears in the stage with start years between 1930 and 1960. It is clear that the DEMLT differences between T_{max} and T_{min} have two major stages. In the first stage, the T_{max} warming rate is larger than that for T_{min} between the DEMLTs of 1901–1930 and 1930–1960. In the second stage, the T_{max} warming rate is lower than that of T_{min} between the DEMLTs of 1930–1960 and 1974–2014. Therefore, the global DTR shows an increasing trend in the first stage and a decreasing trend in the second stage. Figure 4a also reveals that the global DTR trend changed from dramatically decreasing to slightly decreasing around 1940–1969 in the second stage. The DTR DEMLT shows almost no change in the most recent 40 years. Similar to the 30-year DEMLT, the 50-year DEMLT for the globe also shows two major stages for T_{max} and T_{min}. A negative DEMLT appeared in the stage with start years between 1915 and 1965. In general, the 30- and 50-year DTR DEMLTs show that the DTR trend has changed from increasing to decreasing and that the change rate of DTR slightly decreased in the past 5 decades.

3.3 Spatial variation patterns for different periods

The percentage of grid boxes with positive (red bars) and negative (blue bars) DTR trends are shown in Fig. 5a. It can be seen that the percentage of grid boxes with a negative DTR trend is above 50% on most of the timescales

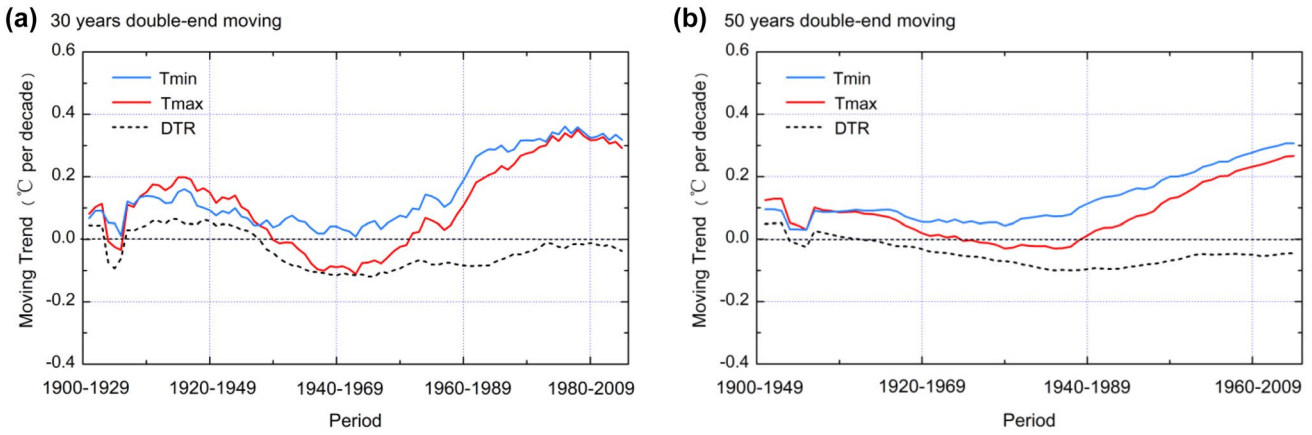

Fig. 4 **a** 30-year and **b** 50-year DEMLTs of annual mean T_{max} (red curves), T_{min} (blue curves), and DTR (black dotted curves) for the globe. Values above zero indicate an increasing trend; values below zero indicate a decreasing trend. For example, the first value of the 30-year DEMLT **a** indicates the linear trend in the period 1901–1930

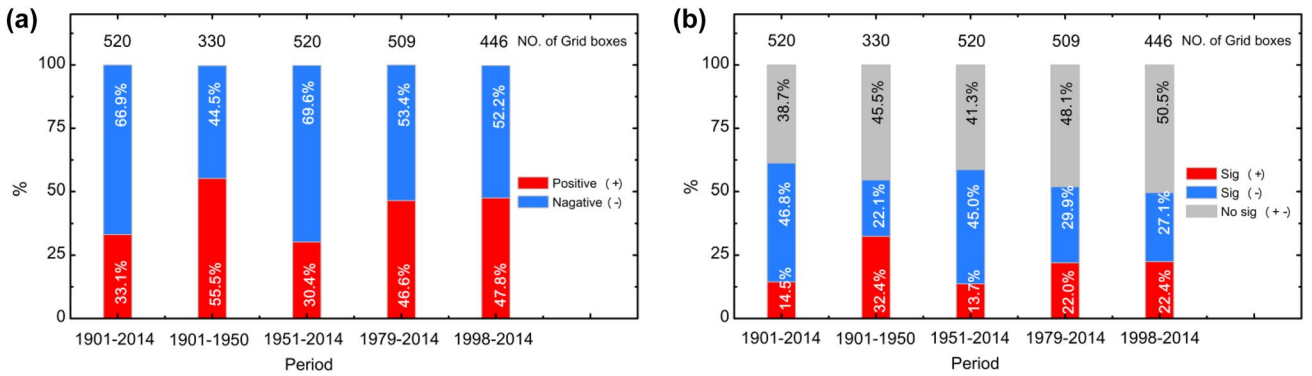

Fig. 5 **a** Percentage of grid boxes with positive (red bars) and negative (blue bars) DTR trends. **b** Percentage of grid boxes with significant positive trends (red bars), significant negative trends (blue bars), and no significant trends (gray bars) in DTR at a confidence level of 95% ($P<0.05$). Numbers in bars with different colors indicate the percentages. Numbers above the bars indicate the number of grid boxes with a spatial resolution of 5°×5°

analyzed, except the period 1901–1950. For 1901–2014 and 1951–2014, the percentage of grid boxes with a negative DTR trend is more than 65%. For 1901–1950, the percentage of grid boxes with a negative DTR trend is 44.5%. Remarkably, there are only 330 grid boxes in the period 1901–1950, which means that the results for this period are more uncertain than those for other periods. For 1979–2014, the percentage of grid boxes with a negative DTR trend (46.6%) is slightly lower than those with a positive DTR trend (53.4%). For the period 1998–2014, the percentages of grid boxes with negative or positive trends exhibit similar rates as in the period 1979–2014.

The percentages of grid boxes with significant positive and negative trends and no significant trends in DTR at a confidence level of 95% are shown in Fig. 5b. Over time, 50% of the grid boxes show statistically significant increasing and decreasing trends in all of the different periods. For the entire study period, 46.8% of the grid boxes show a significant negative trend, while only 14.5% of the grid boxes show a significant increasing trend. For the period 1901–1950, 32.4% of the grid boxes show a significant positive trend, and only 22.1% show a significant negative trend. The percentages of grid boxes with significant negative and positive trends during 1951–2014 are consistent with those for the entire study period. For 1979–2014 and 1998–2014, the percentage of grid boxes with significant trends totals approximately 50%, while there are approximately 22% of grid boxes with significant positive trends.

Overall, the decreasing DTR over the entire study period is mainly due to the obvious decrease in DTR from 1951 to 2014. In 1901–1950, more grid boxes show a positive trend (55.5%), and most of the positive trends are statistically significant (32.4%), which leads to a significant increase in DTR before 1950.

The spatial distribution of annual mean DTR trends during 1901–2014 is shown in Fig. 6a. For the entire study

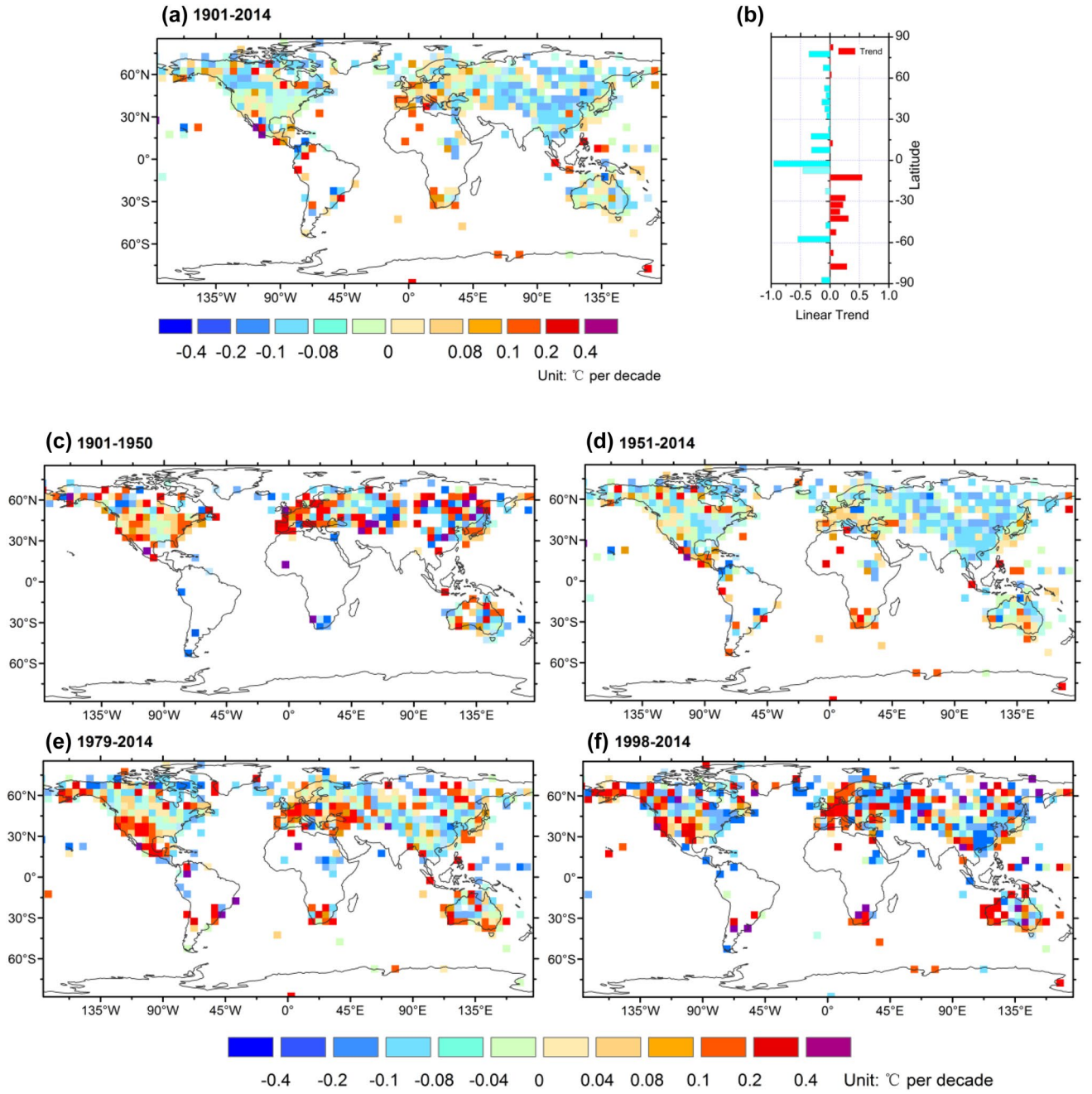

Fig. 6 Global DTR trends in specific periods: **a** 1901–2014, **c** 1901–1950, **d** 1951–2014, **e** 1979–2014, and **f** 1998–2014. **b** The zonal average trends for every 5° of latitude from 1901 to 2014

period, DTR decreased over most areas of the world, with notable dramatic decreases in Asia, North America, and Australia. In most parts of Europe, DTR shows an increasing trend. The zonal average trends for every 5° of latitude are shown in Fig. 6b. The largest annual change corresponding to a decrease in DTR is around the Equator. The decreased areas in DTR are mainly distributed in the NH, while the obvious increasing trends are mainly distributed in the SH. Additionally larger uncertainties are seen in the SH zonal average trends than those in the NH, and the reason can be mainly attributed to fewer grid boxes in the SH than in the NH.

For the period 1901–1950 (Fig. 6c), the DTR in the Northern Hemisphere shows a significant increasing trend, especially in East Asia and Europe. Africa and South America show a downward trend, while Central and Northern Australia shows an increasing trend. For the period 1951–2014, major changes in global DTR show decreasing

trends (Fig. 6d). In this period, most of the grid boxes show a decreasing trend, especially in the NH. Antarctica shows an increasing trend, but it has few grid boxes. Therefore, the global DTR shows an increasing trend in the first half of the last century and a decreasing trend in the second half, once again indicating that an obvious reversal phenomenon occurred around the early 1950s. In 1979–2014, most grid boxes in North America, Europe, Africa, South America, Antarctic, and Western Australia show an obvious increasing trend (Fig. 6e). Asia and Eastern North America exhibit widespread decreases in DTR, although the trend pattern for global DTR is generally mixed. The trends during 1998–2014 exhibit a similar pattern for the period 1979–2014 (Fig. 6f). However, the trend of increasing or decreasing DTR at grid scale is more obvious.

In general, for global DTR, most grid boxes show an obvious decreasing trend during 1901–2014, and an obvious reversal phenomenon around the early 1950s. In addition, the trends of increasing and decreasing global DTR in 1979–2014 and 1998–2014 were more obvious than in other periods.

4 Discussion

4.1 Long-term changes in global DTR

Because of poor observational data, there are few studies focused on the change of DTR on the century scale. Our analysis indicates that global DTR showed a decreasing trend in the 1900–2014 period based on more than 4,000 stations around the World, with a decreasing rate of − 0.036 °C decade^{-1}. Based on data from 524 stations, which were mainly concentrated in North America, Europe, and Australia, Wang and Dickinson (2013) concluded that global and hemispheric DTR showed a downward trend in the period 1900–2010. They also indicated that the main reason for long-term variations is the change of solar radiation reaching the surface, and the impact of solar radiation was − 0.011 °C decade^{-1} from 1900 to 2010.

For the past 6 decades, the quality of global data has been greatly improved, and the changes in DTR have attracted increased attention from researchers. The results in our study are generally consistent with the results achieved by previous studies made over past 6 decades (e.g. Karl et al. 1993; Vose et al. 2005; Easterling et al. 1997; IPCC 2013). These studies used different data sets and base periods, but they consistently show significant decreasing trends in global DTR since the early 1950s, but with different decrease rates. Based on multiple global temperature datasets, Thorne et al. (2016) recently indicated that globally averaged annual mean DTR had decreased since the 1950s or 1960s but that this decrease had not been linear.

The research periods in the studies of Easterling et al. (1997) and Karl and Steurer (1990) are concentrated from the early 1950s to the early 1990s. We choose the results of the Vose et al. (2005) to compare with our results (Sect. 3.1) (Table 1). In general, different results consistently show significant decreasing trends in global DTR since the early 1950s. In the results of Vose et al. (2005), however, global and NH DTR showed more obvious decreasing trends. The major reason is that T_{max} and T_{min} temperature changes tend to be consistent after 2000, resulting in the value of global DTR change to gradually become smaller. The data coverage in the SH is poor, so the results there always have more uncertainty than those in the NH.

In addition to the trend features, a reversal phenomenon was found around 1979 in the studies of Easterling et al. (1997) and Vose et al. (2005) for the period 1951–2004. Owing to the short observation period, the reversal phenomenon did not attract much attention. Makowski et al. (2008) analyzed the changes in DTR in Europe and found that the long-term decreasing trend of DTR in Western Europe began to reverse in the 1970s, while the reversal phenomenon in Eastern Europe occurred in the 1980s. Furthermore, Makowski et al. (2008) also indicated that the reversal phenomenon in Europe occurred in summer and autumn. Based on the new observational dataset, we analyze the changes in DTR for a longer period, 1901–2014, and we find an obvious reversal phenomenon in DTR around the early 1950s, when the trend changes from increasing to decreasing in most parts of the World. The MK test and polynomial fitting are used to detect the trend change and abrupt point of the global DTR series (Fig. 7a, b). Figure 7a shows that global DTR shows a significant increasing trend from the 1930s to the end of the 1950s, and turns to a significant downward trend after the 1970s. Figure 7a also shows that a significant abrupt point occurred in 1978. The MK test could not detect the trend-reversal phenomenon around the early 1950s, but this reversal phenomenon also can be clearly found from the polynomial fitting of the global DTR series (Fig. 7b). Figure 7b shows that the reversal phenomenon around the early 1950s is more obvious than those at other times. This phenomenon is also demonstrated in the series of 30- and

Table 1 Comparison of global DTR changes of the globe, NH, and SH between Vose et al. (2005) and the present paper

References	Data set	Period	Trend (°C decade^{-1})		
			Global	NH	SH
Vose et al. (2005)	GHCN[a]	1950–2004	− 0.066	− 0.076	− 0.033
This paper	CMA-LSAT	1951–2014	− 0.054	− 0.066	0.011

[a]Global Historical Climatology Network data set (Peterson and Vose 1997)

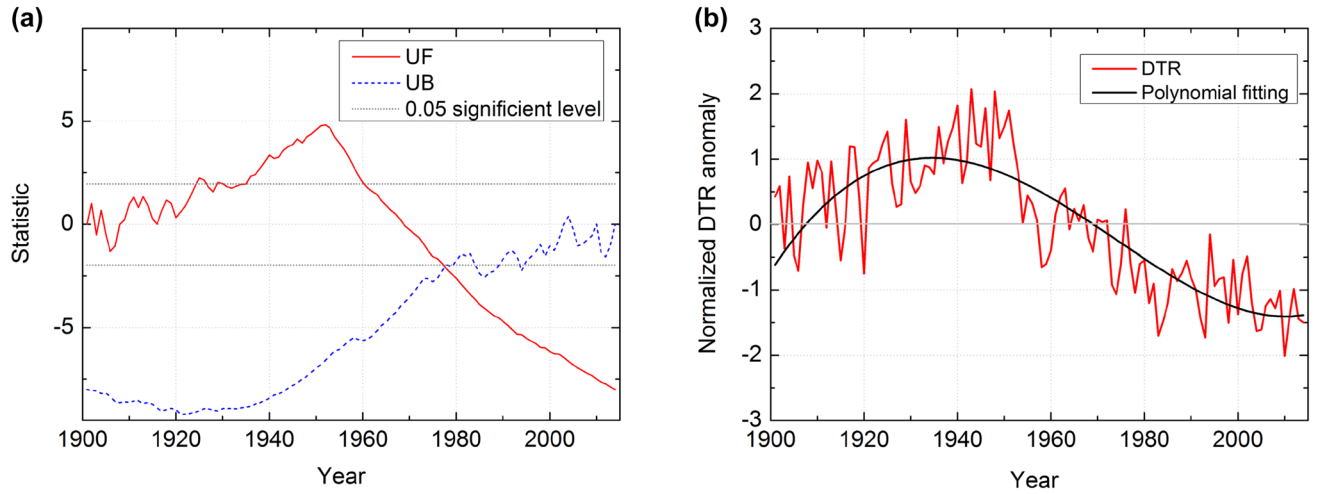

Fig. 7 **a** MK test and **b** polynomial fitting results of global annual mean normalized DTR anomaly series from 1901 to 2014

50-year moving trends. The reversal phenomenon in the NH is consistent with the global DTR pattern and it is statistically significant. In contrast, the reversal phenomenon does not occur in the SH.

4.2 Causes of the long-term changes in global DTR

Previous studies indicated that the long-term changes in cloudiness, precipitation, soil moisture, aerosols, terrestrial vegetation, and local urbanization processes would all play a role in decreasing global DTR since 1951 (e.g. Dai et al. 1999; Zhou and Hansen 2004, 2008; Wild et al. 2005, 2007; Ren et al. 2014). In the recent time periods of 1951–2014 and 1979–2014, southern Europe, northern Africa, the western Middle East, as well as the southwestern United States exhibit obvious increasing DTR trends, which are rather different from the global average. The positive trends have been related to the decrease in cloudiness and precipitation and the increasing drought frequency in these regions (IPCC 2013). The significant decrease in DTR over mainland China and other Asian developing countries might have been mainly caused by the regional dimming resulting from increasing aerosols (Wang and Dickinson 2013; Shen et al. 2015) and rapid urbanization around the observational stations (e.g. Zhou and Ren 2011; Wang et al. 2012; Ren et al. 2006, 2014).

However, due to the lack of observational data and the poor credibility of the observations in the first half of the twentieth century, there are only very few studies focused on the cause of the decreasing trend of global DTR, and few reports are available to analyze the possible causes of the reversal phenomenon around the early 1950s. Table 2 summarizes the previous observational studies reporting trends of the influential factors of DTR in the first half of the twentieth century.

Surface solar radiation (SSR) is considered to play a prominent role in influencing global and regional DTR (Makowski et al. 2009). Since SSR is only present during the day, it could affect T_{max} more than T_{min} (Wild et al. 2007; Makowski et al. 2009). A large number of studies on global and regional "brightening" and "dimming" after 1951 demonstrated that changes in global and regional DTR mainly depend on changes in SSR (e.g. Wild 2009; Makowski et al. 2009; Wild et al. 2008; Long et al. 2009; Che et al. 2005; Qian et al. 2007). However, because of the poor early SSR observational data, there are only a very few studies focused on time series of directly observed SSR for the first half of the twentieth century. Romanou et al. (2007) simulated global SSR in the twentieth century using nine models and found that global SSR showed a decreasing trend over the entire twentieth century. Wild (2009) investigated the SSR data from the longest observational record in Stockholm (Europe) and indicated that there were two "global brightening" periods in the twentieth century, one at the end of the century, and a second one before the 1940s ("early brightening") (Table 2). This can effectively support the DTR reversal phenomenon in Europe that occurred around the early 1950s.

In addition to the most direct SSR factor, another major factor affecting DTR variation is generally recognized to be precipitation. Dai et al. (1997) investigated the relationship between precipitation and DTR and indicated that increased precipitation may have contributed to a DTR decrease by increased evaporative cooling. A more obvious correlation between DTR and precipitation in Europe, North America, and Australia from 1901 to 1990 was also indicated, with the correlation coefficients all above 0.55 in these areas.

Table 2 Summary of the previous studies reporting trends of the influential factors of DTR in the first half of the twentieth century

References	Region	Data sources	Trend increase or decrease (period)		
SSR					
Wild et al. (2009)	Europe(Stockholm)	GEBA[a]	**Increase** (1923–1940 s)	**Decrease** (1950–2002)	n/a
Precipitation					
Present paper	Northern Hemisphere	CMA-GHP[b]	Decrease (1901–1950)	**Increase** (1951–2014)	**Increase** (1901–2014)
TCC					
Henderson-Sellers (1989, 1992), Croke et al. (1999), Sanchez-Lorenzo et al. (2012), Dai et al. (1999, 2006)	North America	Surface-based observations	**Increase** (1901–1950 s)	**Increase** (1960s–1999)	**Increase** (1900–1999)
Lough et al. (1983), Henderson-Sellers (1992)	Europe	Surface-based observations	**Increase** (1901–1940 s)	**Decrease** (1950s–1987)	**Increase** (1900–1987)
Jones and Henderson-Sellers (1992)	Australia	Historical records of Australia	Decrease (1910–1930 s)	**Increase** (1930s–1989)	**Increase** (1910–1989)
Warren et al. (2007)	South America	EECRA[c]	n/a	**Decrease** (1971–1996)	**Decrease** (1971–1996)
	Africa		n/a	Decrease (1971–1996)	Decrease (1971–1996)
Xia (2010)	China	CMA-Monthly TCC	n/a	**Decrease** (1955–2005)	
Volcanic					
Wang et al. (2014)	Global	SIGVP[d]	Increase (1901–1950)	**Increase** (1950–2010)	**Increase** (1901–2010)

All of the following studies are based on observational data

Black bold fonts represent a statistically significant trend

[a]Global energy balance archive

[b]China Meteorological Administration—Global Historic Monthly Mean Precipitation Dataset

[c]Extended edited cloud reports archive

[d]Smithsonian Institution Global Volcanic Program

The changes of total cloud cover (TCC) are the main reason for the variability of long- and short-wave radiation at land surfaces (Sanchez-Lorenzo et al. 2012). The TCC and DTR have been proved to have a good correlation in some parts of the World after the 1950s (Dai et al. 1999), except for some regions such as South America, Africa (Warren et al. 2007), China (Xia 2010), and Italy (Maugeri et al. 2001). Observational TCC records mainly began being recorded in the mid-eighteenth century in Europe, North America, and Australia. Table 2 shows the TCC changes in different regions, including some details of the reviewed publications. In Europe, the TCC trend showed a significant increase before the 1940s, decreased significantly after the 1950s and became increasing after the 1970s (Lough et al. 1983; Henderson-Sellers 1989). These studies therefore could not support the global and regional DTR changes since 1901. Dai et al. (1999) found that the correlation coefficient between total cloud cover and DTR was very low in Europe, and the correlation coefficient was lower than 0.35 from 1900 to 1990. In Australia, TCC also showed a general increasing trend from 1910 to 1989, with the main increase having occurred in the 1930s to the 1980s (Jones and Henderson-Sellers 1992). In North America, previous studies confirmed that TCC has increased in a fluctuating way from 1900 to the 1980s, as the major increase occurred around the 1930s–1950s and 1960s–1980s (Henderson-Sellers 1989, 1992; Croke et al. 1999; Sanchez-Lorenzo et al. 2012). These studies could not support the reversal DTR phenomenon in North America around the early 1950s. However, Karl and Steurer (1990) indicated that the period of increasing TCC in the 1930s–1950s in North America can be mainly attributed to biases in observation methodology and observational environments, although the increasing trend after the 1950s has higher reliability. Sanchez-Lorenzo et al. (2012) indicated that traditional TCC observations lack objectivity. Changes in observational environment, observational experience, observation times, and observers can cause TCC series inhomogeneity. Therefore, due to the low credibility of early TCC observations, the changes in

DTR before the early 1950s cannot be explained by the changes in total cloud coverage.

Volcanic eruption can affect land-surface air temperature by reducing solar radiation (Robock 2000). Robock (2000) indicated that five kinds of volcanic eruption indexes showed increasing trends from 1901 to 2000, although the change was not significant. It was also found that the volcanic intensity showed a significant decreasing trend from the 1960s to 2000. Based on Smithsonian Institution global volcanic program data, Wang et al. (2014) also indicated that the large volcanic eruption events showed an increasing trend during 1901–2010. These previous studies indicated that the increase of both volcanic eruption frequency and volcanic eruption intensity could partly explain the long-term decrease of global DTR since 1901.

In addition to the above factors that affect changes in DTR, aerosol, water vapor, and land use changes would be also important. Huang et al. (2006) simulated the interaction between aerosols and clouds and indicated that aerosols led to the decrease of DTR in East Asia since 1950. Makowski et al. (2008) confirmed that there is a significant correlation between SO_2 levels and DTR change in European countries. By analyzing the meteorological data observed after 1950, Kalnay and Cai (2003) pointed out that 50% of the DTR decrease in America in the second half of the twentieth century was caused by changes in land use (including local urbanization). Dai et al. (1999) analyzed the relationship between water vapor and DTR and indicated that water vapor does not have a significant effect on DTR change relative to cloud cover and other factors. None of above factors has credible observational records since 1901, so it is very difficult to analyze the effect of these factors on DTR trends in the first half of the twentieth century.

In general, due to the lack of observational data and the poor credibility of observations in the first half of the twentieth century, it is difficult to assess the causes for the increase in DTR before the early 1950s. Based on the CMA–GHP dataset, we analyzed the relationship between precipitation series and long-term DTR variation in the NH (Fig. 8). Because DTR reversal occurs mainly in the NH, we only calculated the correspondence between the normalized DTR series and normalized precipitation series in the NH (a total of 412 5° × 5° grid boxes). Figure 8 shows that there is a significant negative correlation between precipitation and DTR in the NH, with a correlation coefficient of −0.61. Precipitation in the NH decreased before the early 1950s, while the trend after the early 1950s has increased. Overall, precipitation data could strongly support the DTR reversal phenomenon occurring around the 1950s. Because precipitation is generally accompanied by clouds, the TCC over the global lands may have also increased, which, together with precipitation, may have contributed to the decline of the global and regional DTR. The larger increasing trend

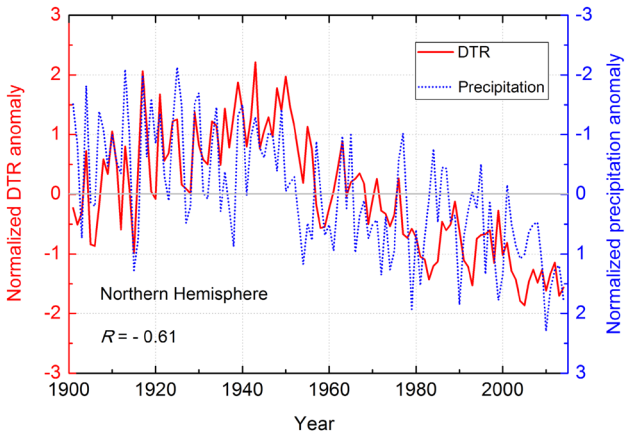

Fig. 8 Variations of normalized anomaly of NH DTR series (red solid line) and precipitation series (blue dashed line) from 1901 to 2014 (relative to 1961–1990). The number represents the correlation coefficient *R*. To compare the two normalized series more easily, the *Y* axis of the precipitation series is placed upside down

Table 3 Trend in DTR for stations with long-term records and all the stations in different periods, along with percentage errors

Period	1901–1950	1951–2014	1901–2014
DTR			
≥ 100 years stations (°C decade^{-1})	0.059	− 0.034	−0.024
All stations (°C decade^{-1})	0.048	− 0.054	−0.036
Percentage errors (%)	23.403	37.421	35.187

of annual precipitation based on the CMA–GHP dataset, as compared to those based on other global precipitation data, needs to be confirmed in the following works, but it is partly supported by a recent analysis of Asian continent, the largest continent of the world (Zhan et al. 2018).

4.3 Uncertainties

Our results are limited by several uncertainties. The major uncertainty is related to DTR calculated using the monthly temperature data. If there are no missing data, the results would be similar to those using daily data. Most observational data used in this study have a relatively long and high-quality record history, especially after 1960. However, the station spatial coverage is poor for the period 1901–1950, which results in the uncertainty of the calculated results. Table 3 shows the DTR trend for stations with long-term records and all stations in three different periods along with the percentage errors. The DTR trends based on the different station networks show consistent patterns of change, but with different magnitudes. The results also clearly show that the differences in DTR trends between long-term record

stations and all stations are at the same level of magnitude. The percentage error for the entire study period is approximately 35%, which is lower than that for 1951–2014 (37%). Before the 1950s, stations with long-term records account for a larger proportion of all stations, which reduces the percentage error to approximately 23%. Therefore, the findings of the DTR reversal phenomenon and the continued decreasing trend of DTR in the past century still have a larger reliability, in spite of the uncertainty.

5 Conclusions

Previous studies indicated that global DTR has been greatly reduced since 1951, and that an obvious reversal phenomenon in DTR occurred around the 1970s. At the same time, it is considered that the change of SSR and precipitation is significantly related to the change of DTR after the 1950s. Changes in factors such as land use, cloud cover, and water vapor can explain the change of DTR after the 1950s. Based on the newly developed CMA-LSAT datasets, in this paper we indicate that global DTR has shown a significant decreasing trend since 1901, and obvious reversal phenomena occurred in global and NH DTR in the early 1950s. Furthermore, precipitation, the number of volcanic eruptions, and the "early brightening" of Europe all support the increase of DTR in the first half of the twentieth century. The results of previous studies on total global cloud cover could not, however, support the increase of DTR in the first half of the twentieth century. Main conclusions of our analysis are as follows.

Observations reported in the present study show changes in annual mean T_{max} and T_{min} to be asymmetrical from 1901. Global T_{max} and T_{min} decreased by nearly 1.1 and 1.6 °C between 1901 and 2014, respectively. The warming rate of T_{min} (0.142 °C decade^{-1}) is approximately 1.5 times that of T_{max} (0.100 °C decade^{-1}), which results in a significant decreasing trend in global DTR (– 0.036 °C decade^{-1}). However, DTR shows obvious interdecadal changes. For the first half of the twentieth century, most grid boxes show a positive DTR trend, with the positive trends of 32.4% grid boxes being statistically significant, leading to a large and significant increase of 0.048 °C decade^{-1} in DTR. However, a dramatic reversal in DTR change occurs around the 1950s, with most parts of global lands seeing a shift from increasing to decreasing trends. The change rate of global land mean DTR is − 0.054 °C decade^{-1} in the second half of the twentieth century. There are 45.0% grid boxes during 1951–2014 showing negative trends of statistical significance.

Spatial distribution shows that DTR has decreased over most areas of the World, with notable dramatic decreases in Asia, North America, and Australia between 1901 and 2014. In most parts of Europe, the DTR shows an increasing trend. However, the global DTR change shows a different spatial distribution in different periods. For the period 1901–1950, annual mean DTR in the NH shows a significant increasing trend, especially in East Asia and Europe. For the period 1951–2014, major changes in global DTR show decreasing trends. Therefore, global DTR shows an increasing trend in the first half of the twentieth century and a decreasing trend in the second half, again indicating that an obvious reversal phenomenon occurred around the 1950s. In the periods 1979–2014 and 1998–2014, most grid boxes in North America, Europe, Africa, South America, Antarctica, and Western Australia show obvious increasing trends, but Asia and Eastern North America still exhibit widespread decreases in DTR.

We also find that the reversal phenomenon that occurred around the 1950s, on global and grid scales, is more obvious than those that occurred at other times. This phenomenon is also demonstrated in the series of 30- and 50-year moving trends. The reversal phenomenon in the NH is consistent with the global DTR pattern and is of statistical significance. In contrast, the reversal phenomenon does not occur in the SH. Owing to the lack of observational data and the poor credibility of the observations in the first half of the twentieth century, it is difficult to assess the causes for the increase in DTR before 1951. However, there is a good negative correlation between DTR and precipitation in the NH from 1901 to 2014, with a correlation coefficient of − 0.61. The number of volcanic eruptions can also support the increase of global DTR before 1951. The Stockholm long-term SSR series and the "early brightening" claim based on the data series are also consistent with the European DTR increase before 1951. The robust reasons for the long-term DTR changes obviously require further study.

Acknowledgements This study is financed by the National Key R&D Program of China (Fund No: 2018YFA0605603), China Natural Science Foundation (CNSF) (Fund No: 41575003) and the MOST (Fund No: GYHY201206012).

References

Alexander LV, Zhang X, Peterson TC, Caesar J, Gleason B, Tank AMGK, Haylock M, Collins D, Trewin B, Rahimzadeh F (2006) Global observed changes in daily climate extremes of temperature and precipitation. J Geophys Res 111(D5):1042–1063

Braganza K, Karoly DJ, Arblaster JM (2004) Diurnal temperature range as an index of global climate change during the twentieth century. Geophys Res Lett 31(13):405–407

Che HZ, Shi GY, Zhang XY, Arimoto R, Zhao JQ, Xu L, Wang B, Chen ZH (2005) Analysis of 40 years of solar radiation data from China, 1961–2000. Geophys Res Lett 32:L06803. https://doi.org/10.1029/2004GL022322

Croke MS, Cess RD, Hameed S (1999) Regional cloud cover change associated with 15 global climate change: case studies for three regions of the United States. J Clim 12:2128–2134

Dai A, Genio ADD, Fung IY (1997) Clouds, precipitation and temperature range. Nature 386(6626):665–666
Dai A, Trenberth KE, Karl TR (1999) Effects of clouds, soil moisture, precipitation, and water vapor on diurnal temperature range. J Clim 12(8):2451–2473
Dai A, Karl TR, Sun B, Trenberth KE (2006) Recent trends in cloudiness over the United States: a tale of monitoring inadequacies. Bull Am Meteor Soc 87(5):597–606
Easterling DR, Horton B, Jones PD, Peterson TC, Karl TR, Parker DE, Salinger MJ, Razuvayev V, Plummer N, Jamason P (1997) Maximum and minimum temperature trends for the globe. Science 277(5324):364–367
Easterling DR, Gleason B, Vose RS, Stouffer R (2006) A comparison of model produced maximum and minimum temperature trends with observed trends for the 20th and 21st centuries. In: 18th conference on climate variability and change, Session 5, January 27–February, 2006, Atlanta, USA
Fyfe JC, Gillett NP (2014) Recent observed and simulated warming. Nat Clim Change 4(3):150–151
Fyfe JC, Meehl GA, England MH, Mann ME, Santer BD, Flato GM, Hawkins E, Gillett NP, Xie SP, Yu K (2016) Making sense of the early-2000s warming slowdown. Nat Clim Change 6(3):224–228
Henderson-Sellers A (1989) North American total cloud amount variations this century. Global Planet Change 1:175–194
Henderson-Sellers A (1992) Continental cloudiness changes this century. Geo J 27:255–262
Huang Y, Dickinson R, ChameidesWL (2006) Impact of aerosol indirect effect on surface temperature over East Asia. Proc Natl Acad Sci USA 103(12):4371–4376
Hundecha Y, Bárdossy A (2005) Trends in daily precipitation and temperature extremes across western Germany in the second half of the 20th century. Int J Climatol 25(9):1189–1202
IPCC (2013) Climate change 2013: the physical science basis. In: Stocker TF, Qin D, Plattner G-K, Tignor M, Allen SK, Boschung J, Nauels A, Xia Y, Bex V, Midgley PM (eds) Contribution of Working Group I to the fifth assessment report of the intergovernmental panel on climate change. Cambridge University Press, Cambridge, p 1535. https://doi.org/10.1017/CBO9781107415324
Jaagus J, Briede A, Rimkus E, Remm K (2014) Variability and trends in daily minimum and maximum temperatures and in the diurnal temperature range in Lithuania, Latvia and Estonia in 1951–2010. Theor Appl Climatol 118(1–2):57–68
Jones PA, Hendersonsellers A (1992) Historical records of cloudiness and sunshine in Australia. J Clim 5(3):260–270
Jones PD, Moberg A (2003) Hemispheric and large-scale surface air temperature variations: an extensive revision and an update to 2001. J Clim 16(2):206–223
Jones PD, Osborn TJ, Briffa KR, Folland CK, Horton EB, Alexander LV, Parker DE, Rayner NA (2001) Adjusting for sampling density in grid box land and ocean surface temperature time series. J Geophys Res 106(D4):3371–3380
Kalnay E, Cai M (2003) Impact of urbanization and land-use change on climate. Nature 423(6939):528–531
Karl TR, Steurer PM (1990) Increased cloudiness in the United States during the first half of nthe twentieth century: fact or fiction? Geophys Res Lett 17:1925–1928
Karl TR, Knight RW, Gallo KP, Peterson TC, Jones PD, Kukla G, Plummer N, Razuvayev V, Lindseay J, Charlson RJ (1993) A new perspective on recent global warming: asymmetric trends of daily maximum and minimum temperature. Bull Am Meteor Soc 74(6):1007–1024
Kerr RA (2009) What happened to global warming? Scientists say just wait a bit. Science 326(5949):28–29
Klein Tank AMG, Können GP (2003) Trends in indices of daily temperature and precipitation extremes in Europe, 1946–1999. J Clim 16(22):3665–3680
Kumar KR, Kumar KK, Pant GB (1994) Diurnal asymmetry of surface temperature trends over India. Geophys Res Lett 21(8):677–680
Li Q, Yang S, Xu W, Wang XL, Jones P, Parker D, Zhou L, Feng Y, Gao Y (2015) China experiencing the recent warming hiatus. Geophys Res Lett 42(3):889–898
Long CN, Dutton EG, Augustine JA, Wiscombe W, Wild M, McFarlane SA, Flynn CJ (2009) Significant decadal brightening of down welling shortwave in the continental United States. J Geophys Res 114:D00D06. https://doi.org/10.1029/2008JD011263
Lough JM, Wigley TML, Palutikof JP (1983) Climate and climate impact scenarios for Europe in a warmer world. J Appl Meteorol 22(22):1673–1684
Makowski K, Wild M, Ohmura A (2008) Diurnal temperature range over Europe between 1950 and 2005. Atmos Chem Phys 8(21):6483–6498
Makowski K, Jaeger EB, Chiacchio M, Wild M, Ewen T, Ohmura A (2009) On the relationship between diurnal temperature range and surface solar radiation in Europe. J Geophys Res 114(D10):1–16. https://doi.org/10.1029/2008JD011104
Maugeri M, Bagnati Z, Brunetti M, Nanni T (2001) Trends in Italian total cloud amount, 1951–1996. Geophys Res Lett 28:4551–4554. https://doi.org/10.1029/2001GL013754
Peterson TC, Vose RS (1997) An overview of the global historical climatology network temperature database. Bull Am Meteorol Soc 78(12):2837–2849
Powell EJ, Keim BD (2014) Trends in daily temperature and precipitation extremes for the southeastern United States: 1948–2012. J Clim 28(4):1592–1612
Qian Y, Wang L, Leung LR, Kaiser DP (2007) Variability of solar radiation under cloud-free skies in China: The role of aerosols. Geophys Res Lett 34(12):2111–2121. https://doi.org/10.1029/2006GL028800
Ren G, Zhou Y, Chu Z, Zhou J, Zhang A, Guo J, Liu X (2006) Urbanization effects on observed surface air temperature trends in North China. J Clim 21(6):1333–1348
Ren G, Ren Y, Li Q, Xu W (2014) An overview on global land surface air temperature change. Adv Earth Sci 29(8):934–946 **(in Chinese)**
Ren G, Ren Y, Zhan Y, Sun X, Liu Y, Chen Y, Wang T (2015) Spatial and temporal patterns of precipitation variability over mainland China: II: recent trends. Adv Water Sci 26(4):451–465 **(in Chinese)**
Río SD, Cano-Ortiz A, Herrero L, Penas A (2012) Recent trends in mean maximum and minimum air temperatures over Spain (1961–2006). Theor Appl Climatol 109(3–4):605–626
Robock A (2000) Volcanic eruptions and climate. Rev Geophys 38(2):191–219
Romanou AB, Liepert B, Schmidt GA, Rossow WB, Ruedy RA, Zhang Y (2007) 20th century changes in surface solar irradiance in simulations and observations. Geophys Res Lett 34(5):89–103. https://doi.org/10.1029/2006GL028356
Salinger MJ, Griffiths GM (2001) Trends in New Zealand daily temperature and rainfall extremes. Int J Climatol 21(12):1437–1452
Samba G, Nganga D (2014) Minimum and maximum temperature trends in Congo-Brazzaville: 1932–2010. Atmos Clim Sci 04(3):404–430
Sanchez-Lorenzo A, Calbó J, Wild M (2012) Increasing cloud cover in the 20th century: review and new findings in Spain. Clim Past 8(4):1199–1212
Shen X, Liu B, Li G, Wu Z, Jin Y, Yu P, Zhou D (2015) Spatiotemporal change of diurnal temperature range and its relationship with sunshine duration and precipitation in China. J Geophys Res 119(23):13163–13179
Stone DA, Weaver AJ (2002) Daily maximum and minimum temperature trends in a climate model. Geophys Res Lett 29(9):70-1–70-4

Sun X, Ren G, Bhaka SA, Ren Y, You Q, Zhan Y, Xu Y, Rajbhandari R (2017a) Changes in extreme temperature events over the Hindu Kush Himalaya during 1961–2015. Adv Clim Change Res 8(3):157–165

Sun X, Ren G, Xu W, Li Q, Ren Y (2017b) Global land-surface air temperature change based on the new CMA GLSAT data set. Sci Bull 62(4):236–238

Sun X, Ren G, Ren Y, Fang Y, Liu Y, Xue X, Zhang P (2017c) A remarkable climate warming hiatus over Northeast China since 1998. Theor Appl Climatol. https://doi.org/10.1007/s00704-017-2205-7

Thorne PW, Donat MG, Dunn RJH, Dunn H, Williams CN, Alexander LV, Caesar J, Durre I, Harris I, Hausfather Z, Jones PD, Menne MJ, Rohde R, Vose RS, Davy R, Klein-Tank AMG, Lawrimore JH, Peterson TC, Rennie JJ (2016) Reassessing changes in diurnal temperature range: intercomparison and evaluation of existing global data set estimates. J Geophys Res. https://doi.org/10.1002/2015JD024584

Vose RS, Easterling DR, Gyron G (2005) Maximum and minimum temperature trends for the globe: an update through 2004. Geophys Res Lett. https://doi.org/10.1029/2005GL024379

Wang K, Dickinson RE (2013) Contribution of solar radiation to decadal temperature variability over land. Proc Natl Acad Sci USA 110(37):14877–14882

Wang K, Ye H, Chen F, Xiong Y, Wang C (2012) Urbanization effect on the diurnal temperature range: different roles under solar dimming and brightening. J Clim 25(3):1022–1027

Wang H, Hao Z, Zheng J (2014) Temporal and spatial distribution characteristics of strong volcanic eruption in 1750–2010. Acta Geogr Sin 69(1):134–140 **(in Chinese)**

Warren SG, Eastman RM, Hahn CJ (2007) A survey of changes in cloud cover and cloud types over land from surface. J Clim 20:717–738

Wild M (2008) Decadal changes in surface radiative fluxes and their importance in the context of global climate change. In: Climate Variability and Extremes During the Past 100 Years. Adv. Global Change Res. Ser. Springer, New York

Wild M (2009) How well do IPCC-AR4/CMIP3 climate models simulate global dimming/brightening and twentieth-century daytime and nighttime warming? J Geophys Res 114:D00D11. https://doi.org/10.1029/2008JD011372

Wild M, Gilgen H, Roesch A, Ohmura A, Long CN, Dutton EG, Forgan B, Kallis A, Russak V, Tsvetkov A (2005) From dimming to brightening: decadal changes in solar radiation at Earth's surface. Science 308(5723):847–850

Wild M, Ohmura A, Makowski K (2007) Impact of global dimming and brightening on global warming. Geophys Res Lett 34(4):545–559

Xia X (2010) Spatiotemporal changes in sunshine duration and cloud amount as well as their relationship in China during 1954–2005. J Geophys Res Atmos 115:D00K06. https://doi.org/10.1029/2009JD012879

Xu W, Li Q, Jones P, Wang X, Trewin B, Yang S, Zhu C, Zhai P, Wang J, Vincent L (2017) A new integrated and homogenized global monthly land surface air temperature dataset for the period since 1900. Clim Dyn. https://doi.org/10.1007/s00382-017-3755-1

Yang S, Xu W, Xu Y, Li Q (2016) Development of a global historic monthly mean precipitation dataset. J Meteorol Res 30(2):217–231

Zhai P, Pan X (2003) Trends in temperature extremes during 1951–1999 in China. Geophys Res Lett 30(17):169–172

Zhan YJ, Ren GY, Yang S (2018) Change in precipitation over Asian continent from 1901 to 2016 based on a new multi-source dataset. Clim Res. https://doi.org/10.3354/cr01523

Zhang X, Vincent L, Hogg W, AinNiitsoo (2000) Temperature and precipitation trends in Canada during the 20th century. Atmosphere 38(3):395–429

Zhou L, Hansen JE (2004) Evidence for a significant urbanization effect on climate in China. Proc Natl Acad Sci USA 101(26):9540–9544

Zhou Y, Ren G (2011) Change in extreme temperature event frequency over mainland China, 1961–2008. Clim Res 50(1–2):125–139

Zhou L, Dickinson R, Dirmeyer P, Chen H, Dai Y, Tian Y (2008) Asymmetric response of maximum and minimum temperatures to soil emissivity change over the Northern African Sahel in a GCM. Geophys Res Lett 35(5):1–6. https://doi.org/10.1029/2007GL032953

Zhou L, Dickinson RE, Dirmeyer P, Dai A, Min SK (2009) Spatiotemporal patterns of changes in maximum and minimum temperatures in multi-model simulations. Geophys Res Lett 36:L02702. https://doi.org/10.1029/2008GL036141